Available online at www.sciencedirect.com
ScienceDirect
Journal of the European Ceramic Society 27 (2007) 1571–1577
www.elsevier.com/locate/jeurceramsoc

Influence of ZrO_2 on the crystallization and properties of lithium disilicate glass-ceramics derived from a multi-component system

Elke Apel *, Christian van't Hoen, Volker Rheinberger, Wolfram Höland

Ivoclar Vivadent AG, Bendererstr. 2, FL-9494 Schaan, Liechtenstein

Available online 27 June 2006

Abstract

Lithium disilicate glass-ceramic in the Li_2O–SiO_2–Al_2O_3–K_2O–P_2O_5 system has been investigated by incorporation of ZrO_2. The influence of ZrO_2 on phase formation, microstructure, biaxial flexural strength and translucency were determined. Investigations were carried out by means of differential scanning calorimetry, X-ray diffractometry and scanning electron microscopy. The mechanical strength was measured corresponding to dental norm ISO 6872 and the contrast ratio determined by BS 5612 method. Zirconia influences the crystallization by hampering crystal growth. With the increasing ZrO_2 content, the crystals become smaller. By increasing the crystallization temperature the crystal growth could be improved. The translucency of the glass-ceramic is adjusted by adding ZrO_2. A highly translucent glass-ceramic with a contrast ratio of approx. 0.4 with a high strength microstructure has been developed.

Keywords: Lithium disilicate; Glass ceramics; ZrO_2; Microstructure-final; Strength

1. Introduction

Since the 1990s, efforts to develop biomaterials for restorative dentistry have been concentrated on producing metal-free systems. An important milestone in this respect was reached in the development of glass-ceramics containing leucite ($KAlSi_2O_6$) (Rheinberger[1]). This material is particularly suitable for fabricating single units such as dental inlays, crowns and veneers because of its special optical properties. In the development of biomaterials whose strength surpasses that of leucite glass-ceramics, research was conducted on sintered ceramics as well as glass-ceramics. In the process, a lithium disilicate glass-ceramic demonstrating high strength was produced using sintering technology. The glass-ceramic exhibited strength values of approx. 400 MPa (three-point bending test), which allowed it to be used in the fabrication of anterior dental bridges (Höland et al.,[2] Schweiger et al.[3]).

Recently, a lithium disilicate glass-ceramic in the Li_2O–SiO_2–Al_2O_3–K_2O–P_2O_5 system[4] was developed, which can be used to produce high strength dental restorations in a mechanical shaping process involving CAD-CAM technology. The glass-ceramic was produced according to the method of controlled nucleation and crystallization of the base glasses through heat treatment. Additional processes such as ion exchange reactions were not needed to produce this material. The present study is based on the fundamental research carried out on this materials system, where strength values of ~740 MPa (biaxial) in translucent glass-ceramics were achieved by controlling the crystallization mechanism of Li_2SiO_3 and $Li_2Si_2O_5$. For the present investigation, a base glass in the Li_2O–SiO_2–Al_2O_3–K_2O–P_2O_5 system was selected in which ZrO_2 additions were systematically increased from 0 to 4 wt%. Therefore, the aim of the present study is to show the influence of ZrO_2 on the microstructure and the resulting strength characteristics as well as on the translucency of the glass-ceramic.

In β-eucryptite/β-spodumene/β-quartz glass-ceramics, ZrO_2 is known as nucleating agent. The reaction of ZrO_2 as a nucleating agent was first described by Tashiro and Wada[5] and later by Beall.[6] Therefore, a possible influence of ZrO_2 on nucleation in lithium disilicate glass-ceramics also will be discussed.

2. Experimental

2.1. Glass synthesis and heat treatment

Four glasses of the lithium disilicate multi-component system were prepared by melting. ZrO_2 contents in wt% of 0, 2.00, 2.91

* Corresponding author. Tel.: +423 235 3617; fax: +423 239 4617.
E-mail address: elke.apel@ivoclarvivadent.com (E. Apel).

0955-2219/$ – see front matter © 2006 Elsevier Ltd. All rights reserved.
doi:10.1016/j.jeurceramsoc.2006.04.103

Table 1
Composition of glasses per analysis in wt%

	Glass 1	Glass 2	Glass 3	Glass 4	Error analysis +/-
SiO_2:Li_2O (Mol)	**2.39**	**2.40**	**2.39**	**2.40**	
	Wt%	Wt%	Wt%	Wt%	Wt%
SiO_2	74.37	72.89	72.21	71.40	0.30
K_2O	3.26	3.18	3.16	3.13	0.05
Li_2O	15.44	15.13	14.99	14.79	0.20
Al_2O_3	3.55	3.48	3.45	3.41	0.05
P_2O_5	3.38	3.31	3.28	3.22	0.01
ZrO_2	**0.00**	**2.01**	**2.91**	**4.05**	**0.05**

and 4.00 were studied (Table 1). Glass 1 represents the ZrO_2-free glass as a reference to the ZrO_2 containing Glasses 2–4. Glass 1 was investigated in detail in a separate study by Höland et al.[4]

It is important to note that the molar ratio of SiO_2:Li_2O was 2.39:1 for each composition. Therefore, the examined compositions were non-stochiometric with respect to the molar composition of the lithium disilicate crystalline phase.

The four glasses were crystallized according to two different heat treatment cycles, that is, cycle A: 650 °C/20 min + 850 °C/10 min, cycle B: 700 °C/20 min + 850 °C/10 min. Heat treatment at 650 °C/20 min or 700 °C/20 min represents the first crystallization step. Heat treatment at 850 °C/10 min represents the second crystallization step of the glass-ceramic.

The glasses were prepared by melting the raw materials of silica, lithium carbonate, aluminium oxi-hydroxy hydrate, aluminium metaphosphate, potassium carbonate and zirconia. The mixture was melted in the laboratory in 150-ml Pt–Rh crucibles at 1450 °C/40 min and subsequently produced a glass frit. The glass frit was remelted at 1500 °C/1.5 h to improve homogeneity. Glass blocks (14 mm × 12 mm × 30 mm) were cast and formed. The specimens were annealed at 500 °C/10 min and subsequently cooled to room temperature at a rate of 3–5 K/min. This relaxation process was conducted to release internal stresses and to initiate the nucleation process.

The chemical composition was analyzed using X-ray fluorescence (XRF) with a Siemens SRS 3000. The lithium/lithium oxide content was measured by means of atomic absorption spectrometry (AAS) using a Varian SpectrAA-200.

2.2. Crystal phase analysis, microstructure and properties

In order to obtain an overview of the crystal phase formation of the four glasses dynamic heat treatments were carried out using differential scanning calorimetry (DSC) with a STA 409 PC calorimeter (Netzsch, Germany). For this purpose, a cast glass block was crushed to produce glass granules with an average grain size of 250–450 μm. For a measurement approx. 35 mg of these granules was heat treated in Pt crucibles in a dry nitrogen atmosphere at 10 K/min.

To determine the crystal phases precipitates during annealing all the base glasses were examined in the dynamic heating process using high temperature X-ray diffraction (HT-XRD). Monolithic glass samples measuring 14 mm × 12 mm × 1.8 mm were prepared and annealed at 500 °C/10 min as described in Section 2.1. The measurements were performed using an AXS D5005 diffractometer at temperatures ranging from room temperature to 1200 °C in 20-K steps and 2θ from 10.0 to 60.07° with a measuring time of 0.3 s and a step size of 0.014°. This yielded an average heating rate of approx. 0.5 K/min for the entire temperature range up to 1200 °C. The phases were evaluated with the DIFFRAC^{plus} software (Bruker, Germany) and identified using ICDD patterns. Room-temperature diffraction X-ray diffraction (RT-XRD) scans were prepared for the crystallized specimens of the A and B cycles.

The microstructure of the glass-ceramic were determined by scanning electron microscopy (SEM). For the SEM images, the specimens of the A and B cycles were examined after the first and second crystallization step. The samples were polished with 4000-grit SiC paper and a 1 μm diamond suspension or fractured and subsequently etched with 40% HF vapour for 10–30 s prior

to sputtering with Au. The images were produced using a DSM 962 device (Zeiss, Germany).

The main focus of the investigation of the main properties was to concentrate on biaxial flexural strength and optical properties, such as translucency. After the A and B cycles, samples were prepared from the annealed glass blocks (14 mm × 12 mm × 30 mm) to examine the biaxial flexural strength (according to ISO 6872). After the first crystallization step, three test specimens (diameter = 14 mm, thickness approx. 1.4 mm) were milled from each block using the CEREC system (Sirona) and subsequently subjected to the second crystallization process at 850 °C/10 min. The specimens were finished and polished (20-μm diamond disc/356 N; 600 SiC grinding paper/178 N/120 s and 1000 grinding paper/178 N/120 s/twice). The final thickness of the specimens was 1.20 mm ± 0.2 mm. The biaxial flexural strength was examined on 15 test specimens using an universal testing apparatus Zwick 1456.

In order to measure the contrast ratio one sample each of the four glasses ($t = 2.0 \pm 0.02$ mm) was subjected to cycles A and B and final crystallization and finished and polished to a high gloss (1000 grit SiC). The measurements were performed according to BS5612 (1978) using a Minolta CM-3700d spectrophotometer.

3. Results

3.1. Glass formation

All the melted glasses were transparent and colourless and did not exhibit any phase separation. The analytical values are shown in Table 1. Following crystallization, all the specimens were white and translucent.

3.2. Overview of crystal phase formation

Fig. 1 shows the curves of the DSC analysis of specimens 1–4. Two pronounced crystallization peaks were measured of all four glasses in the range of 300–1050 °C. The first one was in the temperature range of 630–660 °C, the second one at approx. 840 °C (Table 2). The transformation temperature was found to shift to higher temperatures as the content of ZrO_2 increased, from 468 °C for the ZrO_2-free Glass 1 to just above 480 °C at 4 wt% ZrO_2 (Glass 4).

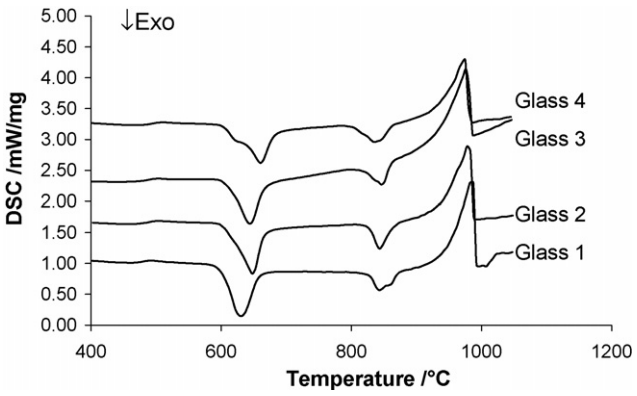

Fig. 1. DSC-graphs of Glasses 1–4, heating rate 10 K/min.

Table 2
Results of DSC-analysis

	Glass 1	Glass 2	Glass 3	Glass 4
T_G (°C)	468.4	477.3	477.0	483.3
DSC (exothermic peak 1) (°C)	630.9	648.4	644.4	660.8
DSC (exothermic peak 2) (°C)	842.7	843.7	847.8	836.7

As shown in a separate study[4] the nucleation, crystal phase formation and solid state reaction of Glass 1 is characterized by heterogeneous nucleation of Li_2SiO_3 and $Li_2Si_2O_5$ by Li_3PO_4. The primary phases were Li_2SiO_3 and $Li_2Si_2O_5$, but growing with different degrees. A high intensity of $Li_2Si_2O_5$ precipitation was determined at 850 °C. In this study a comparison of crystal phase formation of Glasses 2–4 to Glass 1 were made. Fig. 2 shows an evaluation of the HT-XRD diagrams of Glasses 1 and 4, which illustrate the change in the intensities of the main peaks of Li_2SiO_3 and $Li_2Si_2O_5$. Generally, the sequence of crystalline phases was the same in all four glasses.

At temperatures above 520 °C, the crystallization of lithium metasilicate began, reached its maximum at 750 °C and dissoluted above 780 °C. It was accompanied by the crystallization of primarily formed lithium disilicate. $Li_2Si_2O_5$ content remained very low up to a temperature of approx. 750 °C. After that vigorous growth of lithium disilicate started and reached in temperature range of 800–900 °C its maximum.

As the content of ZrO_2 in glasses increased the content of the precipitated crystalline phases remarkable decreased. For example, in Glass 4 smaller amounts of lithium metasilicate and disilicate have been analyzed (Fig. 2). The incorporation of zirconia hampered the crystallization of both phases.

3.3. Phase formation during heat treatment cycles

After both, heat treatment cycles A and B, a phase analysis was carried out using RT-XRD after the first and the second crystallization steps. All crystalline phases were identified in agreement with the phases determined by HT-XRD investigations.

After the first crystallization step, lithium metasilicate was present as the main phase in all the glasses. Additionally

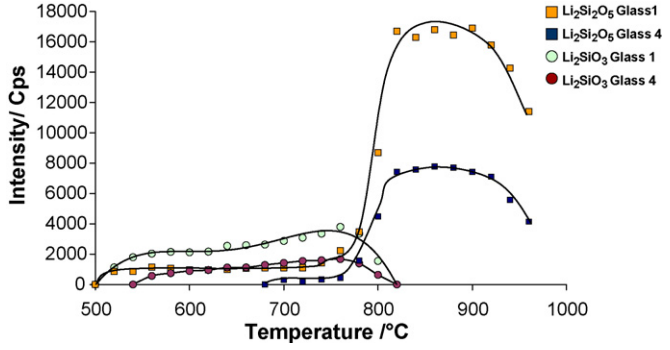

Fig. 2. Results of HT-XRD measurements: Change of intensities of main peaks of Li_2SiO_3 (ICDD-pattern 29-0828, $d = 0.330$ nm) and $Li_2Si_2O_5$ (ICDD-pattern 40-0376, $d = 0.358$ nm).

Table 3
Results of phase analysis, biaxial flexural strength and contrast ratio

	Glass 1	Glass 2	Glass 3	Glass 4
Cycle A: Crystallization step 1 (500 °C/10 min + 650 °C/20 min)				
Intensity (cps) Li_2SiO_3 (29-0828; $d = 0.330$ nm)	9536	6284	4097	3840
Intensity (cps) $Li_2Si_2O_5$ (40-0376; $d = 0.358$ nm)	5339	757	0	0
Cycle B: Crystallization step 1 (500 °C/10 min + 700 °C/20 min)				
Intensity (cps) Li_2SiO_3 (29-0828; $d = 0.330$ nm)	9566	6082	4720	9732
Intensity (cps) $Li_2Si_2O_5$ (40-0376; $d = 0.358$ nm)	5044	686	0	0
Cycle A: Crystallization step 2 (500 °C/10 min + 650 °C/20 min + 850 °C/10 min)				
Intensity (cps) $Li_2Si_2O_5$ (40-0376; $d = 0.358$ nm)	34742	23083	19134	18984
Cycle B: Crystallization step 2 (500 °C/10 min + 700 °C/20 min + 850 °C/10 min)				
Intensity (cps) $Li_2Si_2O_5$ (40-0376; $d = 0.358$ nm)	31969	23201	21414	27089
Biaxial flexural strength (MPa), cycle A	786 ± 92	515 ± 54	522 ± 82	479 ± 36
Biaxial flexural strength (MPa), cycle B	828 ± 104	659 ± 75	608 ± 90	694 ± 113
Contrast ratio, cycle A	0.80	0.56	0.43	0.36
Contrast ratio, cycle B	0.83	0.63	0.53	0.41

$Li_2Si_2O_5$ was detected in Glasses 1 and 2 in small amounts. Table 3 shows the intensities of the main peaks of Li_2SiO_3 ($hkl = 111$; $d = 0.330$ nm) and $Li_2Si_2O_5$ ($hkl = 111$; $d = 0.358$ nm) of the glasses of the A and B cycles from XRD pattern.

In the A cycle, the ZrO_2-free Glass 1 contained the highest amount of Li_2SiO_3 (9536 cps). As the ZrO_2 content increased, the amount of crystalline phase decreased continuously (Glass 4: 3840 cps). Similar results were obtained for the glasses of the B series. But in contrast to cycle A the intensity of Li_2SiO_3 in Glass 4 increased again after heat treatment at 700 °C/20 min. Fig. 3a represents the change in the intensities of the metasilicate as a function of the ZrO_2 content.

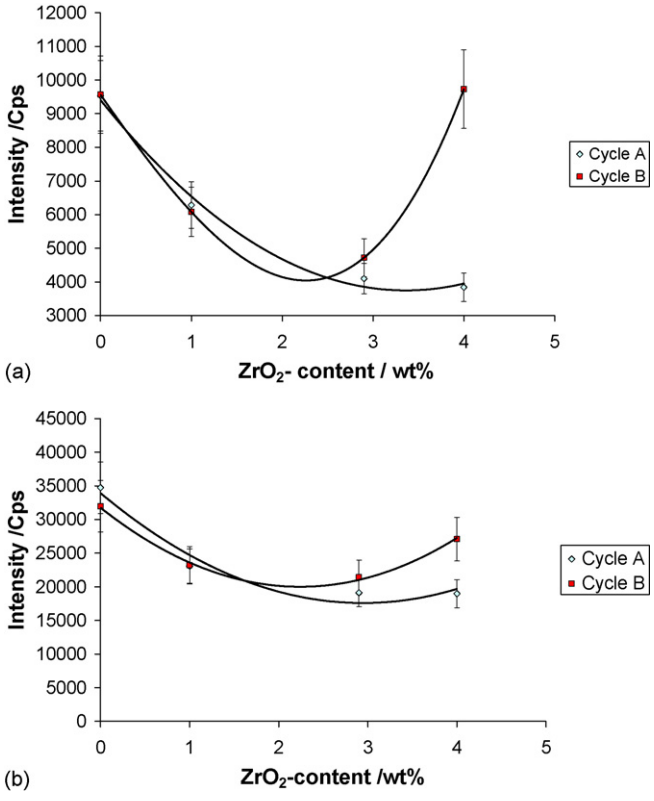

Fig. 3. (a) RT-XRD-measurements: Comparison of intensities of main peaks of Li_2SiO_3 (ICDD-pattern 29-0828, $d = 0.330$ nm) in dependence on ZrO_2 content of cycles A and B. (b) RT-XRD-measurements: Comparison of intensities of main peaks of $Li_2Si_2O_5$ (ICDD-pattern 40-0376, $d = 0.358$ nm) in dependence on ZrO_2 content of heat treatment cycles A and B.

After the second crystallization step at 850 °C/10 min, all the samples contained lithium disilicate as the main crystal phase and Li_3PO_4 as a secondary phase. In a comparison of the intensities of the $Li_2Si_2O_5$ main peaks, a similar relationship with the ZrO_2 content was established as in the metasilicate crystallization (Table 3 and Fig. 3a). With the increasing ZrO_2 content, the crystal content of lithium disilicate decreased by a factor of less than to 2.5 of the base glass in cycle A. In the B series, $Li_2Si_2O_5$ crystallized in the same way as the metasilicate. After dropping to a minimum, the $Li_2Si_2O_5$ content in Glass 4 increased to a high value of 27.000 cps and therefore corresponded to approx. 85% of Glass 1 with 32.000 cps. (Fig. 3b).

3.4. Microstructure

The SEM images after the first crystallization process showed a metasilicate main phase and a nanocrystalline disilicate matrix in all samples. This correlated with the results of the phase analysis. Fig. 4 shows the SEM image of Glass 3 after 650 °C/20 min with the dendritic metasilicate crystals as well as the nanocrystalline matrix.

After the second crystallization step, the glass-ceramic demonstrated a very fine microstructure with many lithium disilicate crystals. The crystals were small, measuring between 0.1 and 1 μm in length and exhibited both a needle-like and a flake-like morphology (A cycles). In the B cycles the final disilicate microstructure was coarser due to the higher crystallization temperature of 700 °C. The crystals were considerably larger (up to three times, max. 3 μm), longish rather than round and they had a larger aspect ratio.

The crystal content of the specimens of both series was very high (approx. 75 vol%) and the residual glass matrix was small (approx. 25 vol%). ZrO_2 influenced the microstructure by ham-

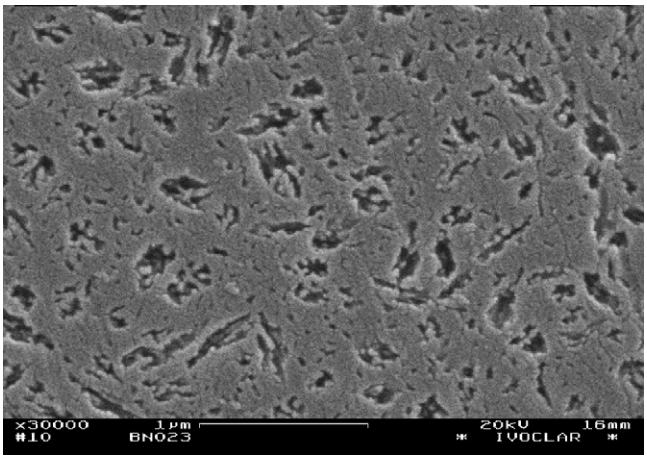

Fig. 4. SEM micrographs of Glass 3 after heat treatment for 650 °C/20 min (cycle A). Lithium metasilicate microstructure and nano-crystalline lithium disilicate matrix. Polished, etched in 30% HF-acid vapour for 10 s.

pering crystal growth. With the increasing ZrO_2 content, the crystals became smaller. The ZrO_2-free Glass 1A had a coarser microstructure (crystals measuring up to 1 μm) than Glass 4A (max. 0.5 μm). Figs. 5 and 6 show the disilicate microstructure of Glass 4 of the A and B cycles after crystallization at 850 °C/10 min. The long disilicate crystals resulting from the higher metasilicate crystallization temperature of 700 °C.

3.5. Properties

The results of the biaxial flexural strength measurements are shown in Table 2. The highest strength of 786 MPa (cycle A) and 828 MPa (cycle B) was measured for Glass 1. A significant dependence on the ZrO_2 content of the strength was shown (Table 3 and Fig. 7). The data trend correlated very well with the intensities of $Li_2Si_2O_5$ (Fig. 3b). With the increasing ZrO_2 content, the mechanical strength decreased. However, the biaxial flexural strength of Glass 4 (cycle B) increased again to a high value of 694 MPa, which translated to 84% of the baseline value

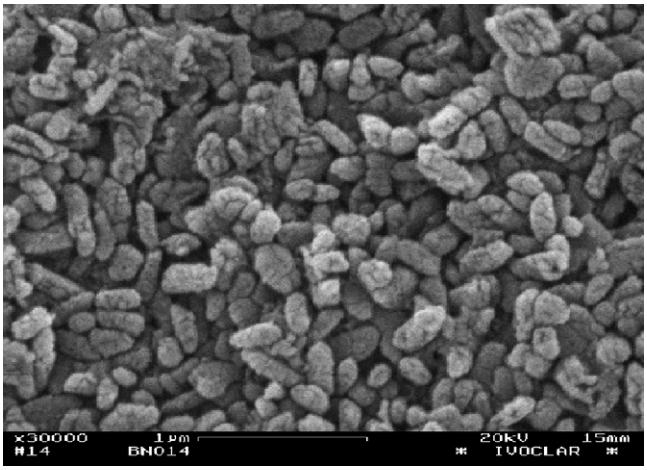

Fig. 5. SEM micrographs of Glass 4 after heat treatment for 650 °C/20 min and 850 °C/10 min (cycle A). Lithium disilicate microstructure, fractured, etched in 30% HF-acid vapour for 30 s.

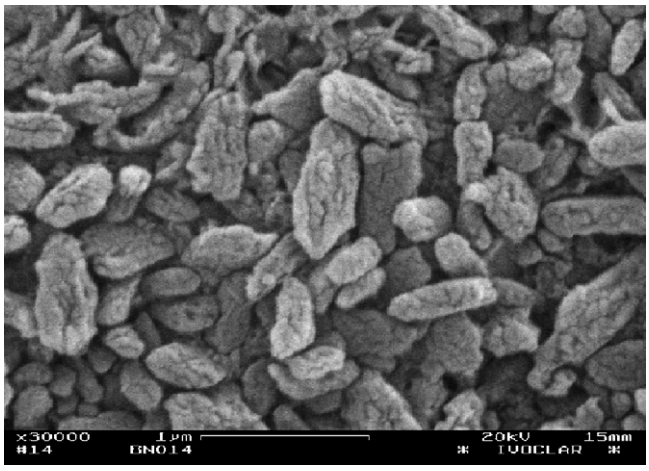

Fig. 6. SEM micrographs of Glass 4 after heat treatment for 700 °C/20 min and 850 °C/10 min (cycle B). Lithium disilicate microstructure, fractured, etched in 30% HF-acid vapour for 30 s.

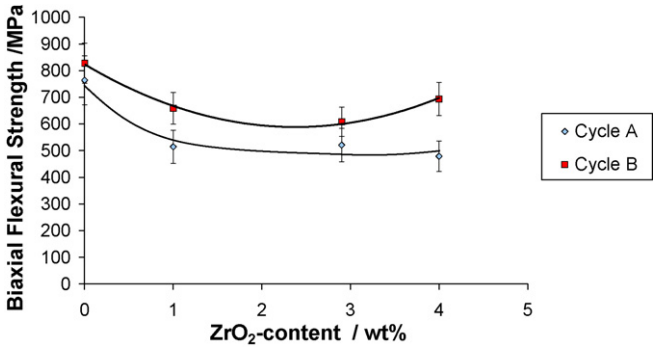

Fig. 7. Biaxial flexural strength (ISO 6872, $n = 15$) in dependence on ZrO_2 content of heat treatment cycles A and B.

of Glass 1B. Thus, the results of the biaxial flexural strength measurements correlate very well with the results of the phase formation analysis.

The contrast ratio (CR) measured for all the specimens of the A and B cycles are shown in Table 3 and graphically represented in Fig. 8. The dependence on the ZrO_2 content as well as the heat treatment (cycles A and B) is clearly recognizable. As the ZrO_2 content increased, the CR values dropped from 0.8 (Glass

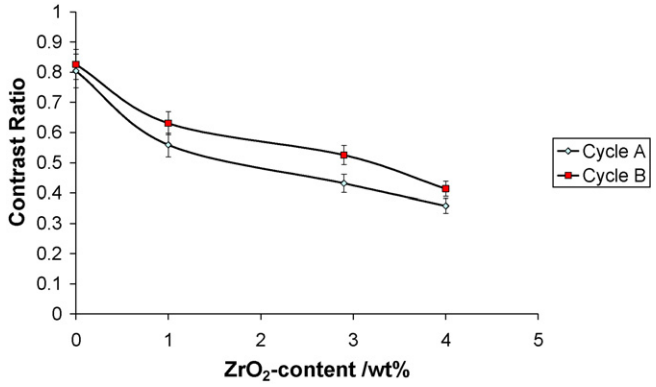

Fig. 8. Contrast ratio (BS 5612) in dependence on ZrO_2 content of heat treatment cycles A and B.

1A) to 0.36 (Glass 4A) and from 0.83 (Glass 1B) to 0.41 (Glass 4B). Thus, the glass-ceramic became more transparent within the respective series. The higher crystallization temperature of metasilicate in the B cycles, which led to a coarser final lithium disilicate microstructure, caused the CR value to rise. Therefore, the opacity of the glass-ceramic increased. Interesting to note Glass 4B with the highest translucency and the longest crystals.

4. Discussion

The aim of the present study was to examine the role of ZrO_2 in phase formation and the resulting properties such as strength and translucency/opacity in the multi-component system. In the glasses of Li_2O–SiO_2–Al_2O_3–K_2O–P_2O_5–ZrO_2 system with the non-stochiometric disilicate composition, Li_2SiO_3 and Li_2SiO_5 crystallize at temperatures above 520 °C, forming coexistent crystalline preliminary phases. The crystallites of lithium disilicate are initially in the nanoscale range (Fig. 4). Vigorous growth of Li_2SiO_5 only sets in above 780 °C (Fig. 2). The phase sequence of disilicate crystallization, which has been described by Höland et al.,[4] was also found when ZrO_2 is added.

As a function of the ZrO_2 content, a slight decline in the content of lithium metasilicate was noted in the A cycles following the crystallization of this phase at 650 °C. This can be explained by an increase in the viscosity, or strengthening the glass network, which results in hampering the growth of lithium metasilicate. If metasilicate crystallization was carried out at 700 °C, more metasilicate crystallized. Therefore, ZrO_2 influenced the crystallization kinetics of the crystal phases.

This was also visible in the disilicate crystallization reaction at 850 °C. In the glasses with the high metasilicate content after the first crystallization step, more disilicate crystallized after the second crystallization step. The data trends in Fig. 3a (metasilicate crystallization) and Fig. 3b (disilicate crystallization) correlate, indicating that the crystallization of $Li_2Si_2O_5$ is linked to that of Li_2SiO_3.

By adding ZrO_2, the content of crystalline Li_2SiO_3 and $Li_2Si_2O_5$ are reduced with exception of Glass 4 (cycles B). In this sample, the content of crystalline phases was comparable to that in ZrO_2-free Base Glass 1 (Fig. 3a and b). The intensities of the $Li_2Si_2O_5$ main peaks of both specimens attained similarly high values of 27.000 cps (Glass 4B) and 32.000 cps (Glass 1B). The reason of this phenomenon could not be clearly established within this study. One explanation could be a change in the structure of the residual glassy matrix, whereby the required diffusion of material is facilitated and the necessary reaction kinetics are initiated. A nucleating effect of ZrO_2 (up to 4 wt%) was not found. The number of crystals after crystallizations seemed not to be increased.

The disilicate microstructure produced after the crystallization process was very fine-scaled. The crystal size ranged between 0.1 and 3 μm. The morphology of the crystals was both needle-like and flake-like (Figs. 5 and 6). The addition of ZrO_2 hampered crystal growth, while the improved metasilicate crystallization at 700 °C promoted it.

As a result of the small size of the crystallites and the increase in the refractive index of the residual glass matrix, the contrast value declined as the ZrO_2 content increased, making the examined samples more translucent. An increase in the metasilicate content after the first crystallization process at 700 °C caused the final microstructure to be more opaque and demonstrate higher contrast values compared with the results after crystallization at 650 °C. The content of the residual glassy matrix after the final crystallization at 850 °C was very low, while the crystal content of $Li_2Si_2O_5$ was approx. 75 vol% (Figs. 5 and 6).

The biaxial flexural strength of the microstructure of Glass 1 reached 786 MPa (A cycles) and 828 MPa (B cycles). A dependence of the strength of the final disilicate microstructure on the content of the previously crystallized metasilicate was established.

The interrelationship between the primary disilicate phase, the maximization of the metasilicate and the crystallization of lithium disilicate produced a highly cross-linked microstructure which contained an isolated residual matrix and resulted in high strength values.

5. Conclusion

We concluded that ZrO_2 influences the reaction kinetics of the crystallization processes of both lithium metasilicate and lithium disilicate. The ZrO_2-free glass-ceramic has a very fine and strong microstructure. The incorporation of ZrO_2 into the glass matrix does not increase in strength. Because of an increase in the viscosity due to a higher ZrO_2 content in the glass-ceramic and the linked reduction in crystal growth of Li_2SiO_3 and $Li_2Si_2O_5$, lower strength values are achieved than in the base glass. However, if the crystallization conditions for Li_2SiO_3 are improved by increasing the crystallization temperature from 650 to 700 °C, the crystallization of $Li_2Si_2O_5$ becomes more vigorous and a coarser microstructure results. This structure demonstrates an increase in strength of up to 200 MPa comparing to heat treatment cycle A and B. The glass-ceramic with 4 wt% ZrO_2 represents a special reaction behaviour and shows higher strength than glass-ceramics with 2.0 wt% or 2.91 wt%.

The addition of ZrO_2 increases the translucent properties of the glass-ceramic. By varying the chemical composition and the crystallization conditions, CR values between 0.35 and 0.80 can be achieved. Therefore, the translucency of this lithium disilicate glass-ceramic can be customized for applications in aesthetic restorative dentistry.

References

1. Rheinberger, V., Perspectives in dental ceramics. *Glastech. Ber. Glass Sci. Technol.*, 1997, **70C**, 339–400.
2. Höland, W., Schweiger, M., Frank, M. and Rheinberger, V., A comparison of the microstructure and properties of the IPS Empress®2 and the IPS Empress® glass-ceramic. *J. Biomed. Mater. Res. (Appl. Biomater.)*, 2000, **53**, 297–303.
3. Schweiger, M., Höland, W., Frank, M., Drescher, H. and Rheinberger, V., IPS Empress®2: a pressable high strength glass-ceramic for esthetic all ceramic restoration. *Quint. Dent. Technol.*, 1999, **22**, 143–152.

4. Höland, W., Apel, E., van't Hoen, C. and Rheinberger, V., Studies of nucleation, primary phase formation and solid state reaction in high strength lithium disilicate glass-ceramics. *J. Non-Cryst. Solid*, in press.
5. Tashiro, T. and Wada, M., Glass-ceramics crystallized with zirconia. *Advances in Glass Technology*. Plenum Press, New York, 1963, p. 18–19.
6. Beall, G. H., Structure, properties and nucleation of glass-ceramics. In *Advances in Nucleation and Crystallization in Glasses*, ed. L. L. Hench and S. W. Freiman. The Am. Ceramic Society, Columbus, OH, USA, 1971, pp. 251–261.